Matrix formulation of the Gaussian expansion of coherent multiple beams in arbitrary dimensions

H. Coïc, Y. Abdelmoumni-Prunes, C. Rouyer, N. Bonod

▶ **To cite this version:**

H. Coïc, Y. Abdelmoumni-Prunes, C. Rouyer, N. Bonod. Matrix formulation of the Gaussian expansion of coherent multiple beams in arbitrary dimensions. Journal of the Optical Society of America. A Optics, Image Science, and Vision, 2024, 41 (3), pp.560. 10.1364/JOSAA.516662 . hal-04703392

HAL Id: hal-04703392
https://hal.science/hal-04703392v1

Submitted on 20 Sep 2024

HAL is a multi-disciplinary open access archive for the deposit and dissemination of scientific research documents, whether they are published or not. The documents may come from teaching and research institutions in France or abroad, or from public or private research centers.

L'archive ouverte pluridisciplinaire **HAL**, est destinée au dépôt et à la diffusion de documents scientifiques de niveau recherche, publiés ou non, émanant des établissements d'enseignement et de recherche français ou étrangers, des laboratoires publics ou privés.

Matrix Formulation of the Gaussian Expansion of Coherent Multiple Beams in Arbitrary Dimensions

H. Coïc[1,*], Y. Abdelmoumni-Prunes[1], C. Rouyer[1], and N. Bonod[2]

[1] CEA-CESTA, F-33116 Le Barp, France
[2] Aix-Marseille Univ, CNRS, Centrale Marseille, Institut Fresnel, Marseille, France
[*] Corresponding author: herve.coic@cea.fr

Compiled September 20, 2024

Modeling the propagation of beams along laser beamlines is very challenging due to the multi-dimensional and multi-scale configuration of the problem. Spatio-temporal couplings are particularly difficult to address with conventional numerical methods. Here we derive the Wigner function of a sum of Gaussian beams by calculating the multi-dimensional Fourier transform of the inter-correlation function of the fields. The matrix formulation allows for a simple propagation of the Wigner function in the framework of matrix optics. The relevancy of this approach is assessed by applying this model to one-dimensional and multi-dimensional configurations and by studying the influence of spatio-temporal couplings when considering propagation and dispersion by a diffraction grating. © 2024 Optica Publishing Group

http://dx.doi.org/10.1364/ao.XX.XXXXXX

1. INTRODUCTION

The recent results on inertial confinement fusion [1], [2] have renewed interest in high-energy and high-power laser beamlines [3]. Laser facilities dedicated to fusion generally operate in the nanosecond regime (NIF [4], LMJ [5], Shenguang III [6]) and are sometimes associated with high-power lasers in the picosecond regime (PETAL [7], ARC [8], Omega EP [9]) for radiography.

The description of the laser propagation in high-energy laser beamlines necessitates a multi-dimensional consideration due to the spatial (x,y), temporal (t) and spectral characteristics of the beams together with its polarization states. A major challenge for accurately modelling the propagation of the laser beams is the significant coupling between these quantities, which drastically complicates the problem. Moreover, the characterization of these beams involves multi-scale couplings. Typically, beams on the LMJ (Mega joule Laser) feature a sub-metric size while an accurate description of the beam requires to model the impacts of sub-millimeter spatial defects [10]. The multi-scale challenge occurs also in high-power laser facilities for which time delays span from a few nanoseconds for stretched beams to sub-picosecond for compressed beams.

Predicting the evolution of high-power or high-energy beams from the source to the focal volume is important to determine the acceptable operating points in order not to damage the beamline, and to evaluate the characteristics of the beam at the focal spot for both nanosecond smoothed beams [11, 12], and picosecond beams [13]. The current models used for high-power lasers are based on the numerical resolution of the nonlinear Schrödinger equations, using the Beam Propagation Method (BPM) principle with multi-step Fourier transform [14], [15]. Numerical calculations to characterize these beams therefore require significant computational resources. Besides, because of the numerical nature of these models, parametric studies of the beamlines require a large number of calculations, which can be prohibitively long.

To avoid these difficulties, one possibility is to characterize the laser beamlines using analytical models, without numerical calculation, and in particular Gaussian beams. In this case, there are no sampling problems related to numerical computation, and the computational support is infinite. Besides, studying the influence of a certain parameter of the beamline on the beam characteristics is straightforward. The expansion of any beam into a sum of Gaussian beams through Gabor expansion [16, 17] allows to generalize the properties of Gaussian fields to arbitrary laser beams. But other modal expansions may be more appropriate.

Associating the Gaussian beam expansion with the Wigner [18, 19] representation of the field, instead of the field itself, allows to avoid Fourier transforms to calculate the beam propagation, which drastically simplifies the computation [20]. Another perk of using the Wigner function is that all linear transformations of the field, e.g. through an $ABCD$ matrix transformation, correspond in the phase-space domain to a simple, linear transformation of the coordinates [21]. Moreover, for Gaussian beams, the Wigner function and its associated projections in the sub-spaces (marginals and moments [22]) are analytic and have a Gaussian representation. This property is particularly relevant in high-power laser beamlines for which beam propagation, focusing or compression can be reduced to linear transformations. The Gabor expansion allows to expand any laser beam into a

sum of Gaussian beams. Its association with the Wigner formalism would allow a simple and accurate description of the fields in space and time domain, but it requires to extend the Wigner function to a sum of coherent Gaussian beams including cross-terms.

The main objective of this paper is to establish the generalized Wigner function for a sum of Gaussian beams. We detail here the Wigner formalism for the propagation of a sum of two Gaussian beams. The multi-dimensional Fourier transform of the intercorrelation function gives the Wigner function in a general form, called cross-term, whose reduced formulation (self-terms) is well known and studied in the literature [23, 24]. The method followed to get the Wigner function for the sum of two Gaussian beams can then easily be applied to a more general expansion with an arbitrary number of beams. We illustrate these results with an application of the model in the mono-dimensional and multi-dimensional cases.

2. GENERALIZED WIGNER FUNCTION FOR GAUSSIAN STRUCTURES

A. Normalized Gaussian field

The most general expression of a Gaussian field can be expressed as follows, for two fields as different as possible [24]:

$$E_0(\mathbf{q}) = \mathcal{E}_0 exp\left[-\frac{1}{2}(\mathbf{q}-\mathbf{q}_0)^T\mathbf{Z}_0(\mathbf{q}-\mathbf{q}_0) + i\mathbf{p}_0^T\mathbf{q} + i\phi_0\right] \quad \textbf{(1a)}$$

$$E_1(\mathbf{q}) = \mathcal{E}_1 exp\left[-\frac{1}{2}(\mathbf{q}-\mathbf{q}_1)^T\mathbf{Z}_1(\mathbf{q}-\mathbf{q}_1) + i\mathbf{p}_1^T\mathbf{q} + i\phi_1\right] \quad \textbf{(1b)}$$

with:

$$Z_0 = \mathbf{U}_0 + i\mathbf{V}_0 \quad \textbf{(2a)}$$

$$Z_1 = \mathbf{U}_1 + i\mathbf{V}_1 \quad \textbf{(2b)}$$

In this expression, $\mathbf{q}$ is a vector of dimension n that represents the coordinates of the field. In the case where $n = 1$, we will restrict ourselves to a single scalar coordinate, spatial or temporal (x or t), whereas for $n = 3$, we will be able to consider simultaneously the coordinates (x, y, t) in the form of a vector. $\mathbf{q}_0$ and $\mathbf{q}_1$ represent the offsets in space and/or in time of each Gaussian function of the field $E_0(\mathbf{q})$ and $E_1(\mathbf{q})$. $\mathbf{p}_0$ and $\mathbf{p}_1$ represent the linear phase shift of the field, which corresponds for example to a tilt in the spatial domain or a spectral shift in the time domain. ϕ_0 and ϕ_1 are the constant phase terms associated to the fields.

The $n \times n$ matrices $\mathbf{U}_0$ and $\mathbf{U}_1$ are real symmetric and positive and contain the quadratic amplitudes of the fields, and will be restricted, in the case $n = 1$, to a scalar quantity, which is the squared inverse of the width of the beam, *e.g.* $U_0 = 1/\Delta x^2$, in the case of a purely spatial treatment. The $n \times n$ matrices $\mathbf{V}_0$ and $\mathbf{V}_1$ are real symmetric and give the quadratic phase contribution of the field.

The normalization factors of the field are given by:

$$\mathcal{E}_0 = \sqrt{\mathbb{E}_0}\frac{Det(Re(\mathbf{Z}_0))^{\frac{1}{4}}}{\pi^{\frac{n}{4}}} \quad \textbf{(3a)}$$

$$\mathcal{E}_1 = \sqrt{\mathbb{E}_1}\frac{Det(Re(\mathbf{Z}_1))^{\frac{1}{4}}}{\pi^{\frac{n}{4}}} \quad \textbf{(3b)}$$

For the normalization of the field, we consider that the fields have a respective energy $\mathbb{E}_0$ and $\mathbb{E}_1$:

$$\mathbb{E}_0 = \int_{-\infty}^{\infty} E_0(\mathbf{q})\, E_0^*(\mathbf{q})\, d\mathbf{q} \quad \textbf{(4a)}$$

$$\mathbb{E}_1 = \int_{-\infty}^{\infty} E_1(\mathbf{q})\, E_1^*(\mathbf{q})\, d\mathbf{q} \quad \textbf{(4b)}$$

B. Matrix expression of the intercorrelation function between the fields

The intercorrelation function $\Gamma_{01}(\mathbf{q}, \mathbf{q}')$ between the fields centered at positions $\mathbf{q} - \mathbf{q}'$ and $\mathbf{q} + \mathbf{q}'$ respectively is given by [25, 26]:

$$\Gamma_{01}(\mathbf{q}, \mathbf{q}') = E_0(\mathbf{q} - \mathbf{q}')\, E_1^*(\mathbf{q} + \mathbf{q}') \quad \textbf{(5)}$$

This formulation is adapted to the Wigner formalism, as the Wigner function corresponds to its multidimensional Fourier transform (see Section 3). Let us introduce the sums (index m) and differences (index d) of the parameters $\mathbf{Z}_i$, $\mathbf{q}_i$ and $\mathbf{p}_i$ (with i$\in \{0;1\}$):

$$\mathbf{Z}_m = \frac{1}{2}(\mathbf{Z}_0 + \mathbf{Z}_1^*),\ \mathbf{Z}_d = \frac{1}{2}(\mathbf{Z}_0 - \mathbf{Z}_1^*) \quad \textbf{(6a)}$$

$$\mathbf{q}_m = \frac{1}{2}(\mathbf{q}_0 + \mathbf{q}_1),\ \mathbf{q}_d = \frac{1}{2}(\mathbf{q}_0 - \mathbf{q}_1) \quad \textbf{(6b)}$$

$$\mathbf{p}_m = \frac{1}{2}(\mathbf{p}_0 + \mathbf{p}_1),\ \mathbf{p}_d = \frac{1}{2}(\mathbf{p}_0 - \mathbf{p}_1) \quad \textbf{(6c)}$$

With these reduced parameters, the intercorrelation function can then be cast into the following matrix form:

$$\Gamma_{01}(\mathbf{q}, \mathbf{q}') = \mathcal{E}_0\mathcal{E}_1 exp\left[-(\mathfrak{q} - \mathfrak{q}_0)^T\mathbb{Z}(\mathfrak{q} - \mathfrak{q}_0) + 2i\mathbb{p}_0^T\mathfrak{q} + i\phi_d\right] \quad \textbf{(7)}$$

with the following quantities:

$$\mathbb{Z} = \begin{bmatrix} \mathbf{Z}_m & \mathbf{Z}_d \\ \mathbf{Z}_d & \mathbf{Z}_m \end{bmatrix},\ \phi_d = \phi_0 - \phi_1, \quad \textbf{(8)}$$

$$\mathfrak{q} = \begin{bmatrix} \mathbf{q} \\ -\mathbf{q}' \end{bmatrix}, \mathfrak{q}_0 = \begin{bmatrix} \mathbf{q}_m \\ \mathbf{q}_d \end{bmatrix}, \mathbb{p}_0 = \begin{bmatrix} \mathbf{p}_d \\ \mathbf{p}_m \end{bmatrix} \quad \textbf{(9)}$$

From the expressions of the fields described with vectors and matrices of dimensions n and $n \times n$, we can calculate the intercorrelation function with vectors and matrices of dimensions $2n$ and $2n \times 2n$ respectively. This is a generalized form of the expression proposed by Bastiaans [23] for the autocorrelation of a Gaussian beam, to the intercorrelation of two beams with additional linear terms.

In the case of the autocorrelation of the $E_0(\mathbf{q})$ field, the parameters will then reduce to:

$$\mathbf{Z}_m = \mathbf{U}_0,\ \mathbf{Z}_d = i\mathbf{V}_0, \quad \textbf{(10a)}$$

$$\mathbf{q}_m = \mathbf{q}_0,\ \mathbf{p}_m = \mathbf{p}_0 \quad \textbf{(10b)}$$

$$\mathbf{q}_d = \mathbf{0},\ \mathbf{p}_d = \mathbf{0},\ \phi_d = 0 \quad \textbf{(10c)}$$

All the linear and constant parameters associated with the differences are then equal to zero and disappear in the autocorrelation function. $\mathbf{Z}_m$ reduces to the quadratic amplitude and $\mathbf{Z}_d$ to the quadratic phase of the field.

C. Gaussian basis expansion

Let us consider the field E_{tot} resulting from the superposition of the Gaussian fields E_0 and E_1 defined in the previous section:

$$E_{tot}(\mathbf{q}) = E_0(\mathbf{q}) + E_1(\mathbf{q}) \quad \textbf{(11)}$$

Its Wigner function can be written as:

$$W_{tot}(\mathbf{q}, \mathbf{p}) = W_{00}(\mathbf{q}, \mathbf{p}) + W_{01}(\mathbf{q}, \mathbf{p}) + W_{10}(\mathbf{q}, \mathbf{p}) + W_{11}(\mathbf{q}, \mathbf{p}), \quad \textbf{(12)}$$

where, for $(i,j) \in \{0,1\}^2$,

$$W_{ij}(\mathbf{q},\mathbf{p}) = \frac{1}{\pi^n}\int_{-\infty}^{\infty} \Gamma_{ij}\left(\mathbf{q},\mathbf{q}'\right) exp\left[2i\mathbf{p}^T\mathbf{q}'\right] d\mathbf{q}'. \quad (13)$$

As $W_{ij}^* = W_{ji}$, the resulting Wigner function can be reduced to:

$$W_{tot}(\mathbf{q},\mathbf{p}) = W_{00}(\mathbf{q},\mathbf{p}) + W_{11}(\mathbf{q},\mathbf{p}) + 2Re(W_{01}(\mathbf{q},\mathbf{p})) \quad (14)$$

Here, W_{00} and W_{11} are the Wigner functions of the individual Gaussian fields E_0 and E_1 respectively, or self-terms, while W_{01} is the cross-term that describes the interference between the two Gaussian fields [27]. In the rest of this section, we will derive the analytical expressions of those terms.

The generalization of the expression of $W_{tot}(\mathbf{r})$ to a sum of N of Gaussian elements is:

$$W_{tot}(\mathbf{r}) = \sum_{i=0}^{N-1} W_{ii}(\mathbf{r}) + \sum_{i=0}^{N-1}\sum_{j=0,j\neq i}^{N-1} W_{ij}(\mathbf{r}), \quad (15)$$

where $\mathbf{r} = [\mathbf{q},\mathbf{p}]^T$ allows a direct use of the Wigner function to the case of an arbitrary field decomposed into a Gaussian basis, for example through a Gabor expansion [16, 17].

3. GENERALIZED WIGNER CROSS-TERM FORMULATION

A. Analytical expression of the Fourier-transform of the intercorrelation function

In this part, we derive the Wigner function associated with the cross-correlation function of the fields through a simple multidimensional Fourier transform. We obtain a compact and normalized matrix expression which describes both the cross-terms and self-terms. This is the basic structure that allows us to exploit the Gaussian expansion.

The Wigner cross-term is given by the multi-dimensional Fourier transform of Γ_{01} with respect to variable $\mathbf{q}'$:

$$W_{01}(\mathbf{q},\mathbf{p}) = \frac{1}{\pi^n}\int_{-\infty}^{\infty} \Gamma_{01}\left(\mathbf{q},\mathbf{q}'\right) exp\left[2i\mathbf{p}^T\mathbf{q}'\right] d\mathbf{q}' \quad (16)$$

The integration requires to group the terms into $\mathbf{q}'$ while adding the complex term $i\mathbf{p}^T\mathbf{q}'$. We can then write, for the integration term of the Wigner function:

$$\begin{aligned}&\Gamma_{01}\left(\mathbf{q},\mathbf{q}'\right) exp\left[2i\mathbf{p}^T\mathbf{q}'\right]\\ &= \mathcal{E}_0\mathcal{E}_1 exp\left[-\mathbf{q}'^T\mathbf{A}_r\mathbf{q}' + \mathbf{B}_r^T\mathbf{q}' + C_r\right]\end{aligned} \quad (17)$$

in this expression, $\mathbf{A}_r$ is a $n \times n$ complex matrix, $\mathbf{B}_r$ is a vector of dimension n and C_r is a scalar. If the field is of dimension n, the Wigner function is of dimension $2n$ and the complex determinant is [28]:

$$\int_{-\infty}^{\infty} exp\left(-\mathbf{r}^T\mathbf{A}_r\mathbf{r} + \mathbf{B}_r^T\mathbf{r}\right) d\mathbf{r} = \sqrt{\frac{\pi^n}{Det(\mathbf{A}_r)}} exp\left(\frac{1}{4}\mathbf{B}_r^T\mathbf{A}_r^{-1}\mathbf{B}_r\right) \quad (18)$$

The explicit expressions for the matrix and vector terms in the exponential function of equation 17 are given by:

$$\mathbf{A}_r = \mathbf{Z}_m \quad (19a)$$

$$\mathbf{B}_r = 2[\mathbf{Z}_d(\mathbf{q}-\mathbf{q}_m) - \mathbf{Z}_m\mathbf{q}_d + i(\mathbf{p}-\mathbf{p}_m)] \quad (19b)$$

$$\begin{aligned}C_r = &-(\mathbf{q}-\mathbf{q}_m)^T\mathbf{Z}_m(\mathbf{q}-\mathbf{q}_m) - \mathbf{q}_d^T\mathbf{Z}_m\mathbf{q}_d\\ &+\mathbf{q}_d^T\mathbf{Z}_d(\mathbf{q}-\mathbf{q}_m)\\ &+(\mathbf{q}-\mathbf{q}_m)^T\mathbf{Z}_d^T\mathbf{q}_d + 2i\mathbf{p}_d^T\mathbf{q} + i\phi_d\end{aligned} \quad (19c)$$

For the integration of the intercorrelation function, with $\mathbf{A}_r^{-1} = \mathbf{Z}_m^{-1}$, $\mathbf{Z}_m^{-1}\mathbf{Z}_m = \mathbf{I}_d$, and also $\mathbf{Z}_m = \mathbf{Z}_m^T$ we obtain:

$$\begin{aligned}C_r + \frac{1}{4}\mathbf{B}_r^T\mathbf{A}_r^{-1}\mathbf{B}_r = &-(\mathbf{q}-\mathbf{q}_m)^T(\mathbf{Z}_m - \mathbf{Z}_d^T\mathbf{Z}_m^{-1}\mathbf{Z}_d)(\mathbf{q}-\mathbf{q}_m)\\ &-(\mathbf{p}-\mathbf{p}_m)^T\mathbf{Z}_m^{-1}(\mathbf{p}-\mathbf{p}_m)\\ &+i(\mathbf{q}-\mathbf{q}_m)^T\mathbf{Z}_d^T\mathbf{Z}_m^{-1}(\mathbf{p}-\mathbf{p}_m)\\ &+i(\mathbf{p}-\mathbf{p}_m)^T\mathbf{Z}_m^{-1}\mathbf{Z}_d(\mathbf{q}-\mathbf{q}_m)\\ &-i(\mathbf{p}-\mathbf{p}_m)^T\mathbf{q}_d - i\mathbf{q}_d^T(\mathbf{p}-\mathbf{p}_m) + 2i\mathbf{p}_d^T\mathbf{q} + i\phi_d\end{aligned} \quad (20)$$

This expression gives the structure of the generalized cross-term Wigner function.

B. Representation in the phase-space coordinates

By applying the integration expression in Eq. 18 for multidimensional Gaussian functions, we obtain the expression of the generalized cross-term in a compact and matricial Gaussian form:

$$\begin{aligned}W_{01}(\mathbf{r}) = \mathbb{C}_{01} exp\Big[&-\left(\mathbf{r}-\mathbf{r}_m\right)^T\mathbf{Q}_{01}\left(\mathbf{r}-\mathbf{r}_m\right)\\ &-2i\boldsymbol{\nu}_d^T\left(\mathbf{r}-\mathbf{r}_{pm}\right) + i\phi_d\Big]\end{aligned} \quad (21)$$

Equation 21 is a key result of this paper. Associated with the normalization term $\mathbb{C}_{01}$ and the cross-term matrix $\mathbf{Q}_{01}$, which are detailed in the following, it gives a general expression applicable to the intercorrelation of Gaussian fields.

Equation 18 shows that the normalization coefficient ahead of the exponential function is given by:

$$\begin{aligned}\mathbb{C}_{01} = \mathbb{C}_{10}^* &= \frac{\mathcal{E}_0\mathcal{E}_1}{\pi^n}\sqrt{\frac{\pi^n}{Det(\mathbf{Z}_m)}}\\ &= \sqrt{2^n\mathbb{E}_0\mathbb{E}_1}\frac{Det(Re(\mathbf{Z}_0))^{\frac{1}{4}}Det(Re(\mathbf{Z}_1))^{\frac{1}{4}}}{\pi^n Det(\mathbf{Z}_0+\mathbf{Z}_1^*)^{\frac{1}{2}}}\end{aligned} \quad (22)$$

where n is the dimension of the direct space and $2\times n$ the dimension of the phase-space. The explicit result of the integration expression in Eq. 18 is given by Eqs. 20. The first four rows in Eq. 20 contain the quadratic terms, and thus the matrix sub-blocks of the matrix $\mathbf{Q}_{01}$. These quadratic terms can be recast into the following matrix form:

$$-(\mathbf{r}-\mathbf{r}_m)^T\mathbf{Q}_{01}(\mathbf{r}-\mathbf{r}_m) \quad (23)$$

with:

$$\mathbf{r} = \begin{bmatrix}\mathbf{q}\\ \mathbf{p}\end{bmatrix},\ \mathbf{r}_m = \begin{bmatrix}\mathbf{q}_m\\ \mathbf{p}_m\end{bmatrix}, \quad (24)$$

$$\mathbf{Q}_{01} = \begin{bmatrix}\mathbf{Z}_m - \mathbf{Z}_d^T\mathbf{Z}_m^{-1}\mathbf{Z}_d & -i\mathbf{Z}_d^T\mathbf{Z}_m^{-1}\\ -i\mathbf{Z}_m^{-1}\mathbf{Z}_d & \mathbf{Z}_m^{-1}\end{bmatrix} \quad (25)$$

This matrix can also be decomposed as follows:

$$\mathbf{Q}_{01} = \mathbf{M}_{-i\mathbf{Z}_d}^T\mathbf{Q}_{\mathbf{Z}_m}\mathbf{M}_{-i\mathbf{Z}_d} \quad (26)$$

with:

$$\mathbf{M}_{\mathbf{Z}} = \begin{bmatrix}1 & 0\\ \mathbf{Z} & 1\end{bmatrix}, \mathbf{Q}_{\mathbf{Z}} = \begin{bmatrix}\mathbf{Z} & 0\\ 0 & \mathbf{Z}^{-1}\end{bmatrix} \quad (27)$$

where $\mathbf{Q}_{\mathbf{Z}}$ is a diagonal matrix with $Det(\mathbf{Q}_{\mathbf{Z}}) = 1$ which contains the intrinsic characteristics of the beam. $\mathbf{M}_{\mathbf{Z}}$ is a triangular

matrix with $Det(\mathbf{M_Z}) = 1$ and has the properties of an $ABCD$ symplectic matrix. Let us notice that the sub-matrices $\mathbf{Z}_m$ and $\mathbf{Z}_d$ can be obtained by the relations

$$\begin{aligned} \mathbf{Z}_m &= \mathbf{Q}_{[2,2]}^{-1} \\ \mathbf{Z}_d &= i\mathbf{Z}_m\mathbf{Q}_{[2,1]} \end{aligned} \tag{28}$$

where $\mathbf{Q}_{[i,j]}$ are the sub-matrices of $\mathbf{Q}_{01}$. The last term of equation 20 contains the linear terms in $\mathbf{q}$ and $\mathbf{p}$ and can also be written as:

$$\begin{aligned} i[-(\mathbf{p}-\mathbf{p}_m)^T\mathbf{q}_d - \mathbf{q}_d^T(\mathbf{p}-\mathbf{p}_m) + 2\mathbf{p}_d^T\mathbf{q} + i\phi_d] \\ = i[-2\boldsymbol{\nu}_d^T(\mathbf{r}-\mathbf{r}_{pm}) + \phi_d] \end{aligned} \tag{29}$$

with now:

$$\boldsymbol{\nu}_d = \begin{bmatrix} -\mathbf{p}_d \\ \mathbf{q}_d \end{bmatrix}, \ \mathbf{r}_{pm} = \begin{bmatrix} \mathbf{0} \\ \mathbf{p}_m \end{bmatrix}, \tag{30}$$

In the one dimension case, if $U_0 = U_1 = U$ and if there is no quadratic phase terms ($V_0 = V_1 = 0$), then the cross-term Wigner function reduces to [29]:

$$\begin{aligned} 2Re(W_{01}(\mathbf{q},\mathbf{p})) = \frac{\sqrt{2\mathbb{E}_0\mathbb{E}_1}}{\pi} exp\left[-(q-q_m)^2U - \frac{(p-p_m)^2}{U}\right] \\ cos\left(2p_d(q-q_m) - 2q_d(p-p_m) + 2p_dq_m + \phi_d\right) \end{aligned} \tag{31}$$

C. Fourier transform of the autocorrelation function: Self-term of the Wigner function

The previous general formulation implicitly contains the case of the self-term which corresponds to the Fourier transform of the autocorrelation function. We have, for the self-term Wigner function $W_{00}(\mathbf{r})$ corresponding to the field $E_0(\mathbf{q})$:

$$\mathbf{r}_m = \mathbf{r}_0 = \begin{bmatrix} \mathbf{q}_0 \\ \mathbf{p}_0 \end{bmatrix}, \boldsymbol{\nu}_d = \begin{bmatrix} \mathbf{0} \\ \mathbf{0} \end{bmatrix} \tag{32}$$

$$\mathbf{Q}_{00} = \begin{bmatrix} \mathbf{U}_0 + \mathbf{V}_0^T\mathbf{U}_0^{-1}\mathbf{V}_0 & \mathbf{V}_0^T\mathbf{U}_0^{-1} \\ \mathbf{U}_0^{-1}\mathbf{V}_0 & \mathbf{U}_0^{-1} \end{bmatrix} \tag{33}$$

this matrix can also be decomposed as follows [21]:

$$\mathbf{Q}_{00} = \mathbf{M}_{\mathbf{V}_0}^T\mathbf{Q}_{\mathbf{U}_0}\mathbf{M}_{\mathbf{V}_0} \tag{34}$$

with the matrix formulation of equation 27. In this case $\mathbf{Q}_{\mathbf{U}_0}$ becomes a real diagonal matrix. $\mathbf{M}_{\mathbf{V}_0}$ is also real, with the structure of an $ABCD$ lens matrix [30]. It shows that the more general gaussian fields (equations 1) can be obtained by the action of a thin lens on a pure real Gaussian field. The final form for the self-term is :

$$W_{00}(\mathbf{r}) = \mathbb{C}_{00}exp\left[-(\mathbf{r}-\mathbf{r}_0)^T\mathbf{Q}_{00}(\mathbf{r}-\mathbf{r}_0)\right] \tag{35}$$

with now:

$$\mathbb{C}_{00} = \frac{\mathbb{E}_0}{\pi^n} \tag{36}$$

The self-term is thus real and positive. We have analogous expressions for $\mathbf{r}_1$, $\mathbf{Q}_{11}$, and $\mathbb{C}_{11}$.

D. Gabor expansion in the multidimensionnal case

In the Gabor expansion of the field [16, 17], the Wigner cross-terms are a particular case of the generalized Wigner function (equation 21). Indeed, it corresponds to the case where the multidimensional Gaussian functions all have the same width ($\mathbf{U}$) and no phase curvature ($\mathbf{V} = \mathbf{0}$)[31]. The common matrix corresponding to the cross-term will be given by:

$$\mathbf{Q}_{ij} = \begin{bmatrix} \mathbf{U} & \mathbf{0} \\ \mathbf{0} & \mathbf{U}^{-1} \end{bmatrix} \tag{37}$$

The free parameters of the Gabor functions will be limited to the linear terms $\mathbf{r}_m$, $\mathbf{r}_{pm}$ and $\boldsymbol{\nu}_d$, which correspond to functions spaced by a constant value in the direct $\mathbf{q}$ and conjugate $\mathbf{p}$ domain, which will be given by:

$$\mathbf{r}_m = \frac{1}{2}\begin{bmatrix} (i+j)\delta q_1 \\ ... \\ (k+l)\delta q_n \\ (g+h)\delta p_1 \\ ... \\ (m+s)\delta p_n \end{bmatrix}, \boldsymbol{\nu}_d = \frac{1}{2}\begin{bmatrix} -(g-h)\delta p_1 \\ ... \\ -(m-s)\delta p_n \\ (i-j)\delta q_1 \\ ... \\ (k-l)\delta q_n \end{bmatrix} \tag{38}$$

where the constants $\delta q_1, .., \delta q_n, \delta p_1, .., \delta p_n$ and weights of each contribution $C_{i,j,..k,l,g,h,..,m,s}$ ($2 \times n$ coefficients) will be given by the modal expansion. The total Wigner function will then be given by:

$$W_{tot} = \sum_i\sum_j..\sum_k\sum_l\sum_g\sum_h..\sum_m\sum_s C_{i,j,..k,l,g,h,..,m,s}W_{i,j,..,k,l,g,h,..m,s} \tag{39}$$

It should be noted that, in the general case, the implementation of this model requires the processing of a large number of components, which, in the case of numerical processing, means having access to substantial numerical resources [32, 33]. However, our first objective is to have analytical formulations that describe the major evolutions of the beam (marginal and moments). We will therefore seek to minimize the number of components involved, and the numerical aspects will be reduced here to the visualization of results (as is the case for the illustrations given in the following sections). In the case of the application of such a model to the numerical processing of any beam, with Gabor-type decompositions for example, no investigations have been made and evaluation work in this direction needs to be carried out. At this stage, we feel that this model is suited to certain specific multi-scale and multi-dimensional cases found in large-scale laser installations. For more conventional cases, other numerical codes are currently very effective [14]. The Gabor expansion corresponds to $2 \times n$ sum of elementary Wigner functions. It is not always, especially in the multidimensional case, the most suitable expansion, as it requires a large number of components.

4. FIRST MARGINALS

Wigner functions are not directly measurable, and the accessible quantities correspond to projections of the Wigner function into subspaces of the total phase space (marginals [34]). The integration of the Wigner function on the conjugate variable $\mathbf{p}$ will give an intensity, while the integration on the direct variable $\mathbf{q}$ will give the spectral power. In the case of Gaussian fields, all

projections will be analytically integrable, with Gaussian structures. It is also possible to obtain other informations such as the moments of the beam by integrating the function over the whole space [35]:

$$< \zeta^k >= \frac{\int_{-\infty}^{+\infty} \zeta^k W(\mathbf{q},\mathbf{p}) d\mathbf{q} d\mathbf{p}}{\int_{-\infty}^{+\infty} W(\mathbf{q},\mathbf{p}) d\mathbf{q} d\mathbf{p}} \tag{40}$$

where ζ is the variable in the $(\mathbf{q},\mathbf{p})$ space corresponding to the calculated moment and k the order of the moment. We can obtain other quantities by integration over a defined subspace. For example, in a one dimensional space (temporal variable t), the instantaneous frequency will be given by [36]:

$$< \omega(t) >= \frac{\int_{-\infty}^{+\infty} \omega W(t,\omega) d\omega}{\int_{-\infty}^{+\infty} W(t,\omega) d\omega} \tag{41}$$

For all these quantities, if the Wigner function is Gaussian, then the integration is analytical. As in the case of the Wigner function, the modal expansion can be declined on all projections (marginals and moments).

In the following parts, we will limit ourselves to the study of the first marginals (intensity and power spectrum), which are the elementary quantities to describe the beam.

A. Intensity calculation

The calculation of the intensity requires integrating the Wigner function on the vector $\mathbf{p}$, which allows us to obtain a function of the residual vector variable $\mathbf{q}$. We must first isolate, in the Wigner function, the constant C_q, independent of the integration variable $\mathbf{p}$, but which can depend on the variable $\mathbf{q}$. This constant C_q can be written in the form:

$$C_q = -(\mathbf{r}_q - \mathbf{r}_m)^T \mathbf{Q}_{01} (\mathbf{r}_q - \mathbf{r}_m) - 2i\boldsymbol{\nu}_d^T (\mathbf{r}_q - \mathbf{r}_{pm}) + i\phi_d \tag{42}$$

with

$$\mathbf{r}_q = \begin{bmatrix} \mathbf{q} \\ \mathbf{0} \end{bmatrix} \tag{43}$$

Let us now study the linear terms in $\mathbf{q}$.The vector $\mathbf{B}_q$ is obtained with Eq. 18 limited to the space dimension of $\mathbf{q}$:

$$\mathbf{B}_q = -2\mathbf{Q}_{[2,1]}(\mathbf{q} - \mathbf{q}_m) + 2\mathbf{Q}_{[2,2]}\mathbf{p}_m - 2i\mathbf{q}_d \tag{44}$$

with (from expression 25):

$$\mathbf{Q}_{01} = \begin{bmatrix} \mathbf{Q}_{[1,1]} & \mathbf{Q}_{[1,2]} \\ \mathbf{Q}_{[2,1]} & \mathbf{Q}_{[2,2]} \end{bmatrix} \tag{45}$$

and with:

$$\mathbf{Q}_{[1,1]} = \mathbf{Z}_m - \mathbf{Z}_d^T \mathbf{Z}_m^{-1} \mathbf{Z}_d \tag{46a}$$
$$\mathbf{Q}_{[1,2]} = -i\mathbf{Z}_d^T \mathbf{Z}_m^{-1} \tag{46b}$$
$$\mathbf{Q}_{[2,1]} = -i\mathbf{Z}_m^{-1} \mathbf{Z}_d \tag{46c}$$
$$\mathbf{Q}_{[2,2]} = \mathbf{Z}_m^{-1} \tag{46d}$$

The vector $\mathbf{B}_q$ is described in the n dimensional subspace. The Wigner function can now be written, as a function of the variable of integration $\mathbf{p}$:

$$W_{01}(\mathbf{q},\mathbf{p}) = \mathbb{C}_{01} exp(-\mathbf{p}^T \mathbf{A}_q \mathbf{p} + \mathbf{B}_q^T \mathbf{p} + C_q) \tag{47}$$

with now $\mathbf{A}_q = \mathbf{Q}_{[2,2]}$. We can then apply the formula of multidimensional Gaussian integration (equation 18) to obtain the intensity:

$$\begin{aligned} I_{01}(\mathbf{q}) &= \int_{-\infty}^{\infty} W_{01}(\mathbf{r}) d\mathbf{p} \\ &= \mathbb{C}_{01} \sqrt{\frac{\pi^n}{Det(\mathbf{Q}_{[2,2]})}} exp\left(\frac{1}{4}\mathbf{B}_q^T \mathbf{Q}_{[2,2]}^{-1} \mathbf{B}_q + C_q\right) \end{aligned} \tag{48}$$

The integration gives here a complex value of the intensity for the general form of the Wigner function. In the case of self-terms (i.e. $\mathbf{q}_d = 0$), this function becomes positive. In the case of crossed terms, it will be necessary to take, as for the Wigner function, $2Re(I_{01}(\mathbf{q}))$. The total intensity is then:

$$I_{tot}(\mathbf{q}) = \sum_{i=0}^{N-1} I_{ii}(\mathbf{q}) + \sum_{i=0}^{N-1} \sum_{j=0, j\neq i}^{N-1} I_{ij}(\mathbf{q}), \tag{49}$$

B. Power spectral density

We can apply the same method to obtain the power spectral density which consists in integrating on the vector variable $\mathbf{q}$. Here, the constant C_p is independent of the integration variable $\mathbf{q}$, but can now depend on the variable $\mathbf{p}$, can be written in an analogous condensed form:

$$C_p = -(\mathbf{r}_p - \mathbf{r}_m)^T \mathbf{Q}_{01} (\mathbf{r}_p - \mathbf{r}_m) - 2i\boldsymbol{\nu}_d^T (\mathbf{r}_p - \mathbf{r}_{pm}) + i\phi_d \tag{50}$$

with now

$$\mathbf{r}_p = \begin{bmatrix} \mathbf{0} \\ \mathbf{p} \end{bmatrix} \tag{51}$$

Here again, we can use for the constant C_p a matrix formulation in the $2 \times n$ dimensions space. The vector $\mathbf{B}_p$ will now be written:

$$\mathbf{B}_p = -2\mathbf{Q}_{[1,2]}(\mathbf{p} - \mathbf{p}_m) + 2\mathbf{Q}_{[1,1]}\mathbf{q}_m + 2i\mathbf{p}_d \tag{52}$$

The vector $\mathbf{B}_p$ corresponding to the linear terms in $\mathbf{q}$ is again described in the n dimensional subspace. The Wigner function can now be written, as a function of the variable of integration $\mathbf{q}$:

$$W_{01}(\mathbf{r}) = \mathbb{C}_{01} exp(-\mathbf{q}^T \mathbf{A}_p \mathbf{q} + \mathbf{B}_p^T \mathbf{q} + C_p) \tag{53}$$

with $\mathbf{A}_p = \mathbf{Q}_{[1,1]}$.

We apply in the same way the integration formula, which gives the expression of the spectral power:

$$\begin{aligned} S_{01}(\mathbf{p}) &= \int_{-\infty}^{\infty} W_{01}(\mathbf{r}) d\mathbf{q} \\ &= \mathbb{C}_{01} \sqrt{\frac{\pi^n}{Det(\mathbf{Q}_{[1,1]})}} exp\left(\frac{1}{4}\mathbf{B}_p^T \mathbf{Q}_{[1,1]}^{-1} \mathbf{B}_p + C_p\right) \end{aligned} \tag{54}$$

The total power spectral density is then:

$$S_{tot}(\mathbf{p}) = \sum_{i=0}^{N-1} S_{ii}(\mathbf{p}) + \sum_{i=0}^{N-1} \sum_{j=0, j\neq i}^{N-1} S_{ij}(\mathbf{p}) \tag{55}$$

5. EVOLUTION OF THE WIGNER FUNCTION WITH LINEAR TRANSFORMATION

A. Evolution with the same matrix transformation for the two Gaussian beams

The major advantage of the Wigner function to model the propagation of laser beams is that its evolution by a linear transformation modeled by a $\mathbf{M}$ matrix corresponds to a linear transformation of its arguments, i.e. $W_{in}(\mathbf{r}) \rightarrow W_{out}(\mathbf{r}) = W_{in}(\mathbf{Mr})$ [21]. Let us also point out that:

$$\begin{aligned} W_{in}(\mathbf{Mr}) &= W_{out}(\mathbf{r}) \\ &= \mathbb{C}_{01} exp\left[-\left(\mathbf{Mr}-\mathbf{r}_m\right)^T \mathbf{Q}_{01}\left(\mathbf{Mr}-\mathbf{r}_m\right) - 2i\boldsymbol{\nu}_d^T\left(\mathbf{Mr}-\mathbf{r}_{pm}\right) + i\phi_d\right] \\ &= \mathbb{C}_{01} exp\left[-\left(\mathbf{r}-\mathbf{r}_m^{'}\right)^T \mathbf{Q}_{01}^{'}\left(\mathbf{r}-\mathbf{r}_m^{'}\right) - 2i\boldsymbol{\nu}_d^{'T}\left(\mathbf{r}-\mathbf{r}_{pm}^{'}\right) + i\phi_d\right] \end{aligned} \tag{56}$$

It can be observed that the structure of the Wigner function that has undergone a linear transformation by the matrix $\mathbf{M}$ is identical to the structure of the initial Wigner function with the following changes:

$$\mathbf{r}_m^{'} = \mathbf{M}^{-1}\mathbf{r}_m \tag{57a}$$

$$\mathbf{r}_{pm}^{'} = \mathbf{M}^{-1}\mathbf{r}_{pm} \tag{57b}$$

$$\boldsymbol{\nu}_d^{'} = \mathbf{M}^T\boldsymbol{\nu}_d \tag{57c}$$

$$\mathbf{Q}_{01}^{'} = \mathbf{M}^T\mathbf{Q}_{01}\mathbf{M} \tag{57d}$$

It is sufficient to redefine the constant terms $\mathbf{r}_m^{'}$, $\mathbf{r}_{pm}^{'}$, $\boldsymbol{\nu}_d^{'}$, and the generalized matrix $\mathbf{Q}_{01}^{'}$ to obtain the new Wigner function. These transformations of the linear terms are essential to handle the propagation of equation 21.

Since the Wigner functions are self-referential, transformations by $ABCD$ matrix do not account for certain modifications to linear terms. Typically, for a transformation corresponding to propagation over a distance z, the beam undergoes a time delay z/c which must be added to the original linear term [32]. The application discussed in Section 7 will illustrate this property.

B. Evolution with different matrix transformation for the two Gaussian beams

In a laser beamline, the beams considered may not always follow the same optical sequence. For example, on the PETAL laser [7], at the end of the beamline, the beam is segmented and injected into four compressors, which may have different alignments, before being recombined on target. In this case, we need to use the parameters of the Wigner function $\mathbf{Q}_{ij}$, $\mathbf{r}_m$, ν_d to find the parameters of the fields $\mathbf{U}_i$, $\mathbf{V}_i$, $\mathbf{q}_i$ and $\mathbf{p}_i$ in order to reconstruct a new Wigner function. This is always possible in the case of Gaussian fields. Indeed, it should be noted that the constant vectors for the self-terms can be found from constant vectors for the cross-terms by the following relations:

$$\mathbf{q}_0 = \mathbf{r}_{m[1]} + \boldsymbol{\nu}_{d[2]},\ \mathbf{q}_1 = \mathbf{r}_{m[1]} - \boldsymbol{\nu}_{d[2]} \tag{58a}$$

$$\mathbf{p}_0 = \mathbf{r}_{m[2]} - \boldsymbol{\nu}_{d[1]},\ \mathbf{p}_1 = \mathbf{r}_{m[2]} + \boldsymbol{\nu}_{d[1]} \tag{58b}$$

It allows to obtains the vectors for the self-terms:

$$\mathbf{r}_0 = \begin{bmatrix} \mathbf{q}_0 \\ \mathbf{p}_0 \end{bmatrix}, \mathbf{r}_1 = \begin{bmatrix} \mathbf{q}_1 \\ \mathbf{p}_1 \end{bmatrix}, \boldsymbol{\nu}_0 = \begin{bmatrix} -\mathbf{p}_0 \\ \mathbf{q}_0 \end{bmatrix}, \boldsymbol{\nu}_1 = \begin{bmatrix} -\mathbf{p}_1 \\ \mathbf{q}_1 \end{bmatrix} \tag{59}$$

In the case where the matrix evolution is different for the two beams:

$$\mathbf{r}_m^{'} = \frac{1}{2}(\mathbf{M}_0^{-1}\mathbf{r}_0 + \mathbf{M}_1^{-1}\mathbf{r}_1),\ \boldsymbol{\nu}_d^{'} = \frac{1}{2}(\mathbf{M}_0^T\boldsymbol{\nu}_0 - \mathbf{M}_1^T\boldsymbol{\nu}_1) \tag{60}$$

In the same way, the sub-matrices $\mathbf{Z}_0$ and $\mathbf{Z}_1$ for the self-terms are obtained from the cross-terms with the following relations:

$$\mathbf{Z}_0 = \mathbf{Z}_m + \mathbf{Z}_d,\ \mathbf{Z}_1 = \mathbf{Z}_m - \mathbf{Z}_d \tag{61}$$

These relations allow to rebuild the original $\mathbf{Q}_{00}$ and $\mathbf{Q}_{11}$ Wigner matrix from the cross-terms. The evolution of the self-terms is given by:

$$\mathbf{Q}_{00}^{'} = \mathbf{M}_0^T\mathbf{Q}_{00}\mathbf{M}_0,\ \mathbf{Q}_{11}^{'} = \mathbf{M}_1^T\mathbf{Q}_{11}\mathbf{M}_1 \tag{62}$$

This expression provides the new sub-matrix self-terms $\mathbf{Z}_0^{'}$ and $\mathbf{Z}_1^{'}$ and, consequently, the new sub-matrix cross-terms $\mathbf{Z}_m^{'}$ and $\mathbf{Z}_d^{'}$ for $\mathbf{Q}_{01}^{'}$.

It is important to note here that, in the general case, for each matrix transformation $\mathbf{M}$, a vector $\mathbf{r}_M$ associated with this transformation must be added. This vector corresponds to the absolute position of the beam in phase space after the transformation $\mathbf{M}$. In this case, the $\mathbf{r} \rightarrow \mathbf{Mr}$ transformation must be replaced by $\mathbf{r} \rightarrow \mathbf{Mr} - \mathbf{r}_M$. For example, in the case of a propagation in vacuum over a distance z, the associated vector is $\mathbf{r}_M = [0, z/c, 0, 0]^T$, where z/c represents the propagation time of the beam. In the case of diffraction by a grating, the associated vector is $\mathbf{r}_M = [0, 0, k_0 sin(\theta_d - \theta_i), 0]^T$, where θ_d represents the diffraction angle of the beam. In the case where we are solely interested in the self-terms, or in the case of a common matrix transformation for both beams (Section 5 A), these absolute position terms have no impact on the result. On the other hand, when we are concerned with beams that follow different matrix evolutions, these terms become important, in particular for the evaluation of the vector ν_d, which accounts for the difference in position of the two beams in the phase space.

6. ILLUSTRATIONS IN THE UNIDIMENSIONNAL CASE

This section aims to illustrate the validity of this Wigner formalism in the spatial, one-dimensional case. Two cases are proposed. The first one is elementary and concerns the sum of two Gaussian beams of same width but with different phase curvature and linear terms. The second concerns the sum of N Gaussian beams of the same width (modal expansion) allowing to model a top-hat beam. In both cases, we represent the Wigner function and the associated marginals before applying a $\mathbf{M}$ matrix transformation of propagation. The illustrations proposed in this paper (Sections 6 and 7) were carried out with a relatively small number of elementary Gaussian components (from 2 to a few dozen). The kernel of the Wigner functions and the marginals are calculated analytically with Maple software. The numerical aspects are therefore reduced here to the visualization of the results in the proposed window, generally around 500x500 points for 2d visualization. Numerical aspects of processing (speed, memory resources) are not optimized, as this is not the purpose of the paper, and will have to be studied and developed specifically for this type of modeling.

A. Wigner representation and associated first marginals

Figure 1 gives the total Wigner function and the associated marginals which corresponds to the interference of two Gaussian beams of equal energy (case one). The study is limited to

the spatial dimension q. We can observe the contribution of the self-terms W_{00} and W_{11} centered in (q_0, p_0) and (q_1, p_1) respectively in the phase space. The cross-term $2Re(W_{01})$ is localized in $(q_m = 0, p_m = 0)$ in the phase space and has alternatively positive and negative values (interference terms).

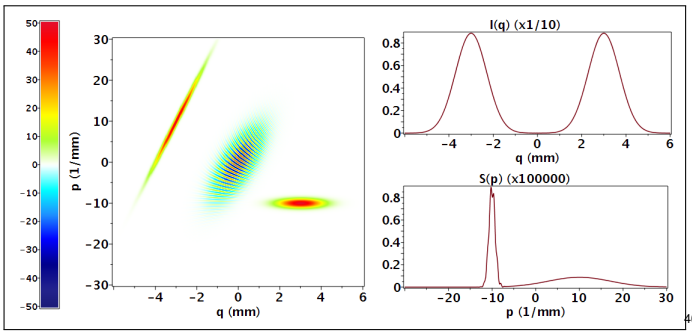

Fig. 1. Representation of the Wigner function $W(q,p) = W(\mathbf{r})$ (left) and the associated marginals $I(q)$ and $S(p)$ (right) for the sum of two Gaussian beams (case one). The beams are defined by, for the first beam $U_0 = 1\,mm^{-2}$, $V_0 = 0\,mm^{-2}$ (no phase curvature), $q_0 = 3\,mm$, $p_0 = -10\,mm^{-1}$ (spatial tilt) and for the second beam $U_1 = 1\,mm^{-2}$, $V_1 = -10\,mm^{-2}$ (divergent beam), $q_1 = -3\,mm$, $p_1 = 10\,mm^{-1}$.

The second application in the spatial domain (case two) is the expansion of a top-hat function (close to Super-Gaussian function) into Gaussian fields (Tovar-type expansion [37]):

$$E(q) = \sum_{n=-N}^{N} E_n(q) = \frac{\sum_{n=-N}^{N} exp\left[-\left(\frac{q-n\delta}{\delta}\right)^2\right]}{\sum_{n=-N}^{N} exp\left[-n^2\right]} \tag{63}$$

where :

$$\delta = \frac{\Delta}{N + \sqrt{1 - ln\left(\sum_{n=-N}^{N} exp\left[-n^2\right]\right)}} \left(\approx \frac{\Delta}{N + 0.653}\ if N > 1\right) \tag{64}$$

denotes both the width and the spacing between the elementary Gaussian beams, and Δ represents the total width of the beam. The order of the corresponding Super-Gaussian beam will be proportional to N, number of contributions taken into account in the calculation. It turns out that the generalized Wigner function has the structure of equation 15 with the parameters of the beam number n : $U_n = \frac{1}{\delta^2}$, $V_n = 0$ (no phase curvature), $q_n = n\delta$, $p_n = 0$. Figure 2 gives the total Wigner function and the associated marginals which corresponds to the addition of the $2N + 1 = 17$ Gaussian beams with $\Delta = 1\,mm$.

B. Evolution of the Wigner function with linear Transformation

Figure 3 gives the total Wigner function and the associated marginals after propagation z for the case one. In the one dimensional case, the transfer matrix $\mathbf{M}$ is :

$$\mathbf{M} = \begin{bmatrix} 1 & -z/k_0 \\ 0 & 1 \end{bmatrix} \tag{65}$$

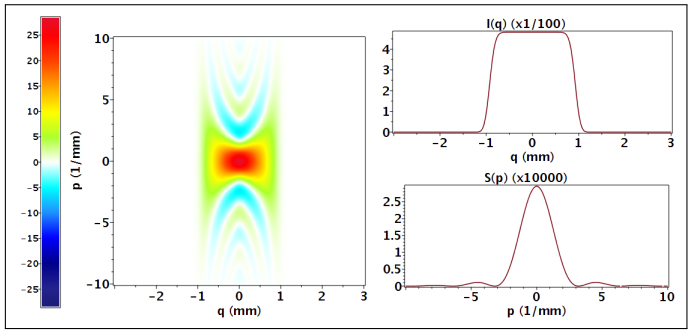

Fig. 2. Representation of the Wigner function $W(q,p) = W(\mathbf{r})$ (left) and the associated marginals $I(q)$ and $S(p)$ (right) for Super-Gaussian beams (case two).

where $k_0 = 2\pi/\lambda$ and λ is the central wavelength ($\lambda = 1.053\,nm$ for the application). The associated Wigner function is simply given by $W'(q,p) = W(\mathbf{Mr})$. For the marginals, we apply the method of Section 4.

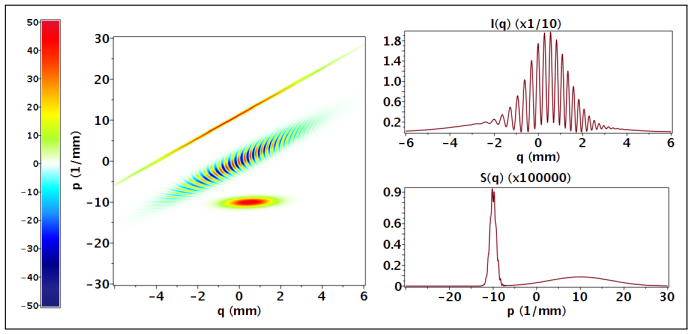

Fig. 3. Representation of the Wigner function $W(\mathbf{Mr})$ (left) and the associated marginals $I(q)$ and $S(p)$ (right) after a propagation distance $z = 1.5\,m$ (case one).

Figure 4 shows the evolution of the intensity I(q) with the variable z for the case one.

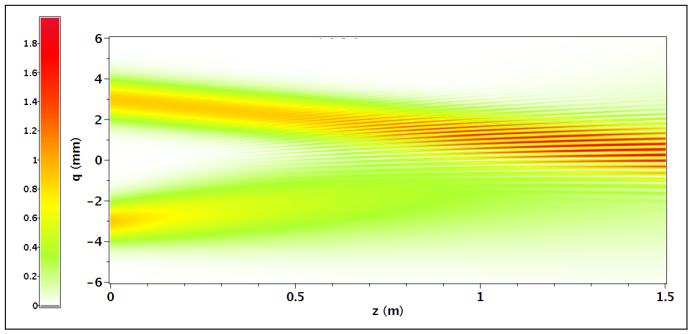

Fig. 4. Evolution of the intensity $I(q)$ of Figure 1 as a function of the propagation distance z (case one).

Figure 5 gives the total Wigner function and the associated marginals after propagation $z = 3\,m$ for the Super-Gaussian beam (case two).

Figure 6 shows the evolution of the intensity I(q) for Super-Gaussian beam with the variable z/k_0 for the case two.

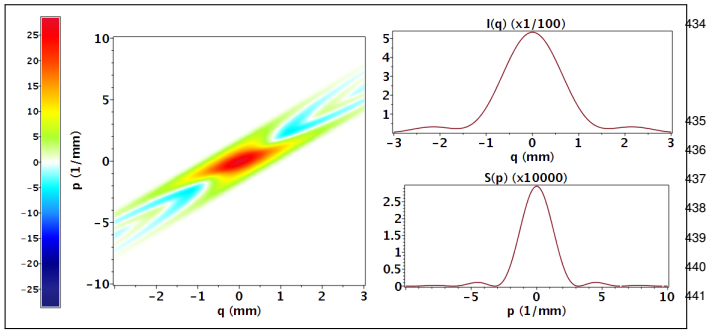

Fig. 5. Representation of the Wigner function $W(\mathbf{Mr})$ (left) and the associated marginals $I(q)$ and $S(p)$ (right) after a propagation distance $z = 3m$ (case two).

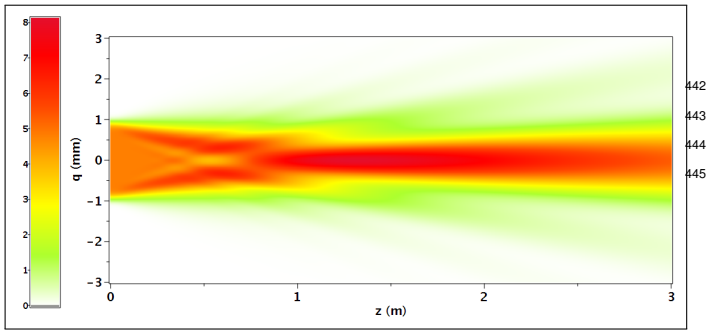

Fig. 6. Evolution of the intensity $I(q)$ of Figure 2 as a function of the propagation distance z (case two).

7. ILLUSTRATION IN THE MULTI-DIMENSIONAL CASE

This section aims to illustrate the multidimensional (spatial and temporal) case with more complex optical transformations, and more specifically propagation and dispersion by a diffraction grating and propagation.

A. Optical scheme analysed

One of the main interests of Wigner functions is their ability to address multi-dimensional and multi-scale cases. To illustrate this property, we consider here a case limited to two-dimensional spatio-temporal (x,t) coordinates. Here, want to model the diffraction of a short pulse with Gaussian temporal envelope and already chirped (phase law<0) by a grating (chirp phase law >0), and study the resulting beam (inhomogeneous wave [38, 39]) as it propagates through a distance z after the grating. To highlight the Gaussian beam expansion of the field, we will use a Tovar-type spatial expansion as studied in section 6. In this case, we consider a spatial expansion on 2N+1=9 elementary Gaussian beams. In the two-dimensional case, the propagation without dispersion and diffraction through a grating matrix are given by [40], [41]:

$$\mathbf{M}_p = \begin{bmatrix} 1 & 0 & -z/k_0 & 0 \\ 0 & 1 & 0 & 0 \\ 0 & 0 & 1 & 0 \\ 0 & 0 & 0 & 1 \end{bmatrix} \mathbf{M}_r = \begin{bmatrix} a & 0 & 0 & 0 \\ -b & 1 & 0 & 0 \\ 0 & 0 & 1/a & -b/a \\ 0 & 0 & 0 & 1 \end{bmatrix} \tag{66}$$

with:

$$a = \frac{cos(\theta_i)}{cos(\theta_d)}, b = \frac{N\lambda}{cos(\theta_d)c}, k_0 = \frac{2\pi}{\lambda} \tag{67}$$

Here, θ_i and θ_d are the incident and diffracted angles, N is the groove density, λ the central wavelength and c is the light velocity. The components of the transformation matrices must respect the order of the selected coordinate system $\mathbf{r} = [\mathbf{q}, \mathbf{p}]^T = [x, t, k_x, \omega]^T$.

The initial parameters of each elementary beam of the spatial expansion before the grating can be given by :

$$\mathbf{U} = \begin{bmatrix} \delta^{-2} & 0 \\ 0 & \Delta t^2/(\Delta t^4 + 16\alpha^2) \end{bmatrix} \quad \mathbf{V} = \begin{bmatrix} 0 & 0 \\ 0 & 4\alpha/(\Delta t^4 + 16\alpha^2) \end{bmatrix} \tag{68}$$

where α is the chirp of the incident beam which corresponds to a phase law $i\alpha\omega^2$ in the spectral domain for the field. Theses parameters allow to build the $\mathbf{Q}_\delta$ matrix for each elementary beam of width δ for the TOVAR-type expansion:

$$\mathbf{Q}_\delta = \begin{bmatrix} \delta^{-2} & 0 & 0 & 0 \\ 0 & \Delta t^{-2} & 0 & 4\alpha/\Delta t^2 \\ 0 & 0 & \delta^2 & 0 \\ 0 & 4\alpha/\Delta t^2 & 0 & (\Delta t^4 + 4\alpha^2)/\Delta t^2 \end{bmatrix} \tag{69}$$

The initial Wigner functions have the same structure as equation 21:

$$W_{ij}(\mathbf{r}) = \mathbb{C}_{01} exp\left[-(\mathbf{r} - \mathbf{r}_m)^T \mathbf{Q}_\delta (\mathbf{r} - \mathbf{r}_m) - 2i\boldsymbol{\nu}_d^T (\mathbf{r} - \mathbf{r}_{pm}) \right] \tag{70}$$

with :

$$\mathbf{r}_m = \begin{bmatrix} \frac{\delta(i+j)}{2} \\ 0 \\ 0 \\ 0 \end{bmatrix}, \mathbf{r}_{pm} = \begin{bmatrix} 0 \\ 0 \\ 0 \\ 0 \end{bmatrix}, \boldsymbol{\nu}_d = \begin{bmatrix} 0 \\ 0 \\ \frac{\delta(i-j)}{2} \\ 0 \end{bmatrix} \tag{71}$$

The Wigner function of the beam after the grating can be obtained as a function of the propagation distance z by applying the matrix transformation on the Wigner function described in Section 5-A with the total matrix sequence $\mathbf{M} = \mathbf{M}_p\mathbf{M}_r$.

B. Visualization and comparison with numerical calculus

Let us represent the first marginals $I(x,t)$ of the initial beam before (figure 7) and just after the grating with a propagation distance $z = 0$ (figure 8). For the application, the spatial and temporal properties of the beams are taken equal to $\delta = 0.322\,mm$ (2N+1=9 elementary Gaussian for the Tovar-type expansion, with a total width $2\Delta = 9mm$), $\Delta t_0 = 300\,fs$. The grating is characterized by its groove density $N = 1740\,g/mm$. The grating is working at Littrow ($\theta_i = \theta_d = 66.363°$) for $\lambda = 1053\,nm$, and its matrix parameters are $a = 1$ and $b = 15.23ns/m$. The initial chirp of the beam is $\alpha = -0.9722ps^{-2}$.

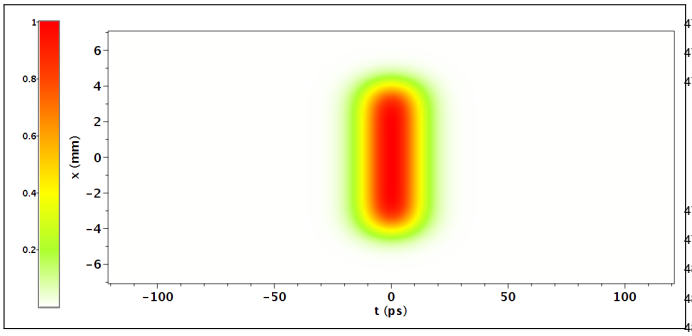

Fig. 7. Representation of the total intensity $I(x,t)$ in spatial and temporal domain of the initial chirped pulse before the grating for a spatially Super-Gaussian and temporally Gaussian beam.

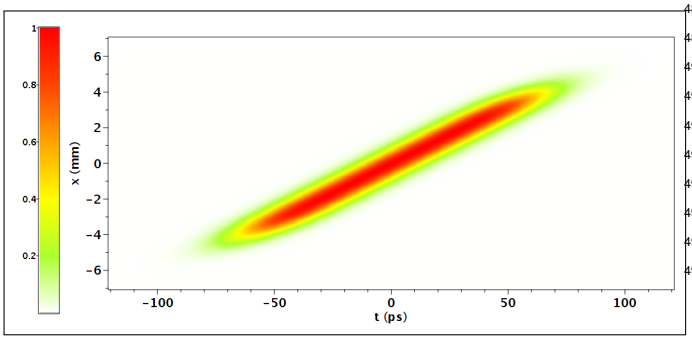

Fig. 8. Representation of the total intensity $I(x,t)$ in spatial and temporal domain just after the grating and without propagation ($z = 0mm$).

Right after the grating, the beam takes the form of an inhomogeneous wave, while retaining its square structure. At this point, it is interesting to plot the fluence of the beam after the grating as a function of the propagation distance z (fig. 9). The square spatial structure of the beam is lost fairly quickly to present a Gaussian spatial structure (spatial to spectral shape transformation) for a propagation greater than $0.5m$. The beam propagation after the grating has a very different structure from that seen in figure 6 for the simple propagation of a top-hat beam. Figure 10

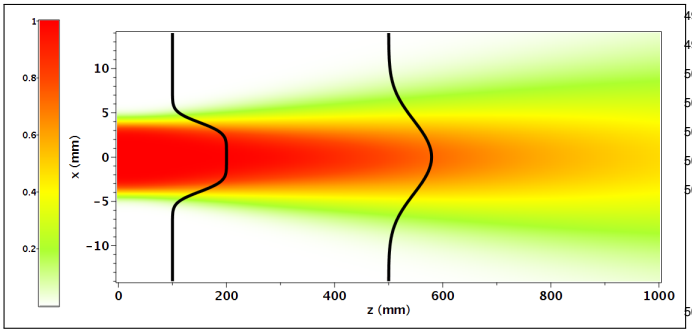

Fig. 9. Fluence of the beam after the grating as a function of the propagation distance z with fluence profile at $z = 100mm$, close to super-Gaussian beam, and at $z = 500mm$, close to Gaussian beam.

represents the intensity of the beam $I(x,t)$ after a propagation $z = 100mm$ at $x = 0$ after the grating. It is the position where the time duration of the beam is minimum (optimal compression of the beam). For a Gaussian beam of width Δx, the distance for the optimal compression is given by:

$$z_0 = \frac{4\alpha\Delta x^2 k_0}{a^2\Delta t^2 + b^2\Delta x^2} \tag{72}$$

This position corresponds also to the plane where a second grating would be positioned to realise a two gratings compressor. In our application, with the numerical values, we have $a^2\Delta t^2/\Delta x^2 << b^2$ and then $z_0 \approx 4\alpha k_0/b^2$ which gives $z_0 \approx 100mm$. At this z position, the beam features a top-hat spatial distribution (figure 9). The advantage of representing short pulse propagation with the Wigner formalism is that the characterization of spatio-temporal distortions (pulse front tilt, wave-front rotation, etc...) can be simply given by combinations of the Wigner function moments [42]. By way of comparison, and as an indication, numerical calculation of the intensity I(x,t) of an inhomogeneous Gaussian wave with z propagation after the grating with dedicated software [14] takes 11" for [x,t]=[512,512] points and 43" for [x,t]=[1024,1024] points. Establishing the formula for the analytical intensity I(x,t,z) with Maple software is almost instantaneous (0.34"), but the display takes 27" for [x,t]=[512,512] points. Application to the flat-top beam (multi-gaussian beam) takes longer to display, due to the sums to be performed on the number of components. But at this stage, performance comparisons with pure numerical code are not really relevant.

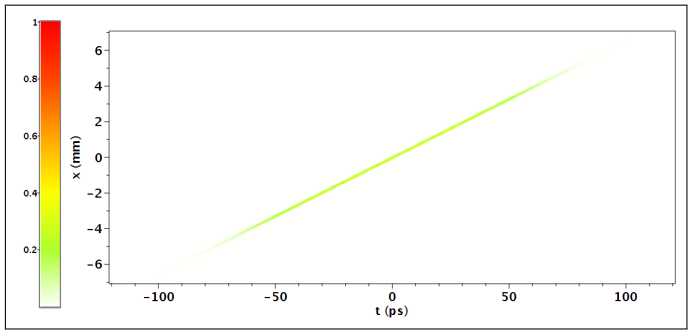

Fig. 10. Representation of the total intensity $I(x,t)$ in spatial and temporal domain in the plane of best compression (propagation $z = z_0 = 100mm$).

Another way of representing the beam is to look at the intensity distribution at a given time as a function of the propagation distance z. In a first approximation, this distribution $I(x,t,z)$ can be given by the visualization of energy density distribution $\rho(x,z;t)$ at each time $t = t_0$, for the incident beam before the grating (in reflection):

$$\rho(x,z;t=t_0) = \frac{1}{c} I(x,t=t_0+z/c;z+ct_0) \tag{73}$$

and by the visualization of:

$$\rho(x,z;t) = \frac{1}{c} I(x,t=t_0-z/c;z-ct_0+3xtan(\theta_d)) \tag{74}$$

for the beam propagating after reflection on the grating. The $3xtan(\theta_d)$ correction on the z coordinate after the grating is necessary to take into account the fact that the grating is slanted and that the position of the incident beam on the grating is at a z coordinate which depends on the x transverse coordinate. The

Wigner formalism does not take this into account. This change of variables transforms an intensity in W/cm^2 in the $2d$ space (x,y) into a volumetric energy density in J/cm^3 in the $3d$ space (x,y,z).

Figure 11 presents, on the same graph, the distribution of energy densities along z at different times and thus at different states of the beam. The beam profile at $z = 36mm$ and time $t_0 = -120ps$ represents the initial chirped beam propagating towards negative z (left arrow). The beam profile at $z = 0mm$ and time $t_1 = 0ps$ and propagating towards z positive (right arrow) is the beam diffracted just after the the grating and presents a structure of inhomogeneous wave ($\theta_{inh} = arctan(cb) = 77.657°$). By convention, the grating is positioned at $z = 0mm$ and is represented by a thick dashed black line at $\theta_d = 66.365°$. The beam profile at $z = 83mm$ and time $t_2 = 276ps$ represents the beam before the optimal compression. Finally, the beam profile at position $z = z_0 = 100mm$ and time $t_3 = 333.3ps$ presents the optimal compression, equivalent to one represented in spatial an time domain in figure 10. The theoretical plane of best compression is represented on the figure by a thin dashed black line centered at $z = 100mm$. All the energy densities are normalised to the energy density at $z = 100mm$ and $x = 0mm$. The behavior of an

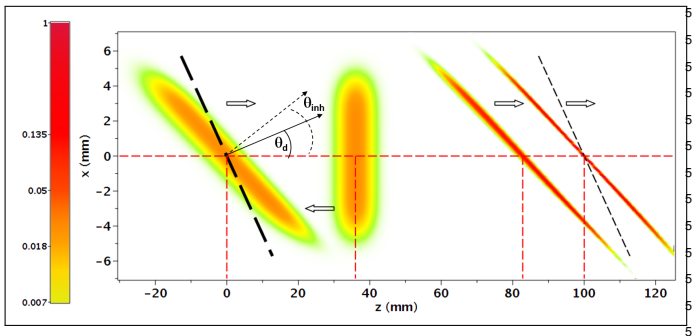

Fig. 11. Energy density distribution of the beam for different times and z position before and after the grating. The beam before the grating (left arrow) is located at $z = 36mm$ at time $t_0 = -120ps$. The diffracted beam are represented by right arrow, in the plane of the grating ($z = 0mm$, $t_1 = 0ps$), before the best plane of compression ($z = 83mm$, $t_2 = 276ps$), and in the best plane of compression ($z = 100mm$, $t_3 = 333.3ps$).

inhomogeneous wave near the best compression plane has been studied and measured [43], showing that the transverse coordinate x of the beam for which compression is maximum is located in the compression plane. To illustrate this, the structure of the compressed pulse near the best compression plane is shown in figure 12 : in the best compression plane centered at $z = 100mm$ at a reference time t_3, the pulse is perfectly compressed at the transverse coordinate $x = 0mm$. For the same inhomogeneous wave at the previous instant (time $t_3 - 34.3ps$), the interception point with the best compression plane is located at the transverse coordinate $x = -4.5mm$ and for the same inhomogeneous wave at the next instant (time $t_3 + 34.3ps$), the best compression plane is located at the transverse coordinate $x = +4.5mm$.
The energy density distribution behavior in a dispersive medium represented in the (x,z) space at a fixed time t and illustrated in figure 12) differs intensity represented in (x,t) space at a fixed spatial longitudinal coordinate z illustrated in figure 10.

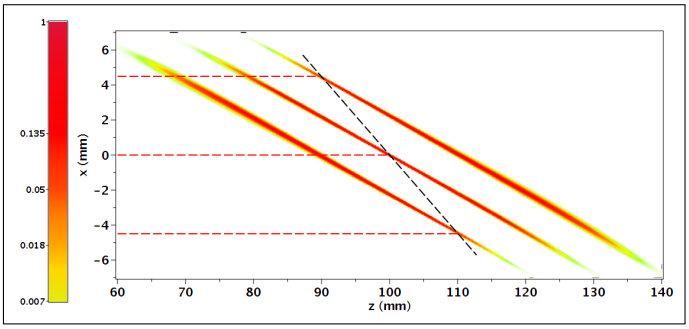

Fig. 12. Energy density distribution of the beam for three different times and z positions around the optimal plane of compression : the beam with a best compression on the transverse coordinate $x = -4.5mm$ at time $t_3 - 34.3ps$, the beam on the plane of best compression at time t_3, and the beam of a best compression on located on the transverse coordinate $x = +4.5mm$ at time $t_3 + 34.3ps$.

8. CONCLUSION

The propagation of laser beams in high-energy laser beamlines is very challenging to simulate with numerical methods due to its multi-dimensional and multi-scale properties. To address this challenge, we propose to develop a Wigner formalism based on a Gaussian expansion of the field. In this study, we derived the expression of the Wigner function corresponding to the sum of two independent Gaussian fields. This formalism, coupled with the Gaussian beam expansion, allows to describe analytically the beams and to model their propagation without limitations related to the numerical resolution. The pertinence and interest of this approach was first evidenced by considering the elementary one-dimensional cases before considering the multidimensional case and coupling effects between the different spaces. This formalism turns out to be very well adapted to model the focal spot in high-energy lasers such as the LMJ-PETAL facility which imply spatio-temporal coupling of smoothed beams (LMJ), compression (PETAL) as well as multi-scale aspects present in particular because of the small typical size of the speckle patterns compared to the envelope of the focal spot. In the latter case, the use of partially incoherent beams (Gaussian Schell Model [23]) in the optical sequence, compatible with the formalism developed in this paper, will provide relevant observables by avoiding an expansion over a large number of Gaussion beams. The formalism is also well adapted to the addition of beams with high angles to model cones at 33° and 49° in the LMJ configuration.This work motivates further developments of the method, in particular the integration of the polarization state of light and the product of fields, which corresponds to the convolution of the Wigner formalism [44]. Indeed, if the correlation is compatible with the linear transformations of the field, convolution of the Wigner functions is the way to deal with nonlinear effects like Kerr effect [45], frequency conversion, spatial filtering [46], or spatial phase mask [47, 48].

Data availability. Data underlying the results presented in this paper are not publicly available at this time but may be obtained from the authors upon reasonable request.

Funding. Commissariat à l'Énergie Atomique et aux Énergies Alternatives.

Disclosure. The authors declare that there are no conflicts of interest related to this article.

REFERENCES

1. A. Kritcher, A. Zylstra, D. Callahan, O. Hurricane, C. Weber, D. Clark, C. Young, J. Ralph, D. Casey, A. Pak *et al.*, "Design of an inertial fusion experiment exceeding the lawson criterion for ignition," Phys. Rev. E **106**, 025201 (2022).
2. A. Zylstra, A. Kritcher, O. Hurricane, D. Callahan, J. Ralph, D. Casey, A. Pak, O. Landen, B. Bachmann, K. Baker *et al.*, "Experimental achievement and signatures of ignition at the national ignition facility," Phys. Rev. E **106**, 025202 (2022).
3. A. Kritcher, A. Zylstra, D. Callahan, O. Hurricane, C. Weber, J. Ralph, D. Casey, A. Pak, K. Baker, B. Bachmann *et al.*, "Achieving record hot spot energies with large hdc implosions on nif in hybrid-e," Phys. Plasmas **28**, 072706 (2021).
4. M. L. Spaeth, K. Manes, D. Kalantar, P. Miller, J. Heebner, E. Bliss, D. Spec, T. Parham, P. Whitman, P. Wegner *et al.*, "Description of the nif laser," Fusion Sci. Technol. **69**, 25–145 (2016).
5. A. Casner, T. Caillaud, S. Darbon, A. Duval, I. Thfouin, J. Jadaud, J. LeBreton, C. Reverdin, B. Rosse, R. Rosch *et al.*, "Lmj/petal laser facility: Overview and opportunities for laboratory astrophysics," High Energy Density Phys. **17**, 2–11 (2015).
6. T. Gong, L. Hao, Z. Li, D. Yang, S. Li, X. Li, L. Guo, S. Zou, Y. Liu, X. Jiang *et al.*, "Recent research progress of laser plasma interactions in shenguang laser facilities," Matter Radiat. at Extrem. **4**, 055202 (2019).
7. N. Blanchot, G. Béhar, J. Chapuis, C. Chappuis, S. Chardavoine, J. Charrier, H. Coïc, C. Damiens-Dupont, J. Duthu, P. Garcia *et al.*, "1.15 pw–850 j compressed beam demonstration using the petal facility," Opt. Express **25**, 16957–16970 (2017).
8. D. Mariscal, T. Ma, S. Wilks, A. Kemp, G. Williams, P. Michel, H. Chen, P. Patel, B. Remington, M. Bowers *et al.*, "First demonstration of arc-accelerated proton beams at the national ignition facility," Phys. Plasmas **26**, 043110 (2019).
9. D. Maywar, J. Kelly, L. Waxer, S. Morse, I. Begishev, J. Bromage, C. Dorrer, J. Edwards, L. Folnsbee, M. Guardalben *et al.*, "Omega ep high-energy petawatt laser: progress and prospects," in *Journal of Physics: Conference Series,* vol. 112 (IOP Publishing, 2008), p. 032007.
10. A. Le Camus, H. Coic, N. Blanchot, S. Bouillet, E. Lavastre, M. Mangeant, C. Rouyer, and J. Néauport, "Impact of compression grating phase modulations on beam over-intensities and downstream optics on petal facility," Opt. Express **30**, 7426–7440 (2022).
11. B. Le Garrec and J. Sajer, "The design of lmj focal spots for indirect drive experiments," in *Journal of Physics: Conference Series,* vol. 112 (IOP Publishing, 2008), p. 032018.
12. A. Bourgeade and B. Nkonga, "Numerical simulations of the focal spot generated by a set of laser beams: Lmj," in *ESAIM: Proceedings,* vol. 32 (EDP Sciences, 2011), pp. 1–17.
13. D. Raffestin, G. Boutoux, N. Blanchot, D. Batani, E. D'Humières, Q. Moreno, T. Longhi, H. Coïc, F. Granet, J. Rault *et al.*, "Application of harmonics imaging to focal spot measurements of the "petal" laser," J. Appl. Phys. **126**, 245902 (2019).
14. O. Morice, "Miró: Complete modeling and software for pulse amplification and propagation in high-power laser systems," Opt. Eng. **42**, 1530–1541 (2003).
15. R. Sacks, K. McCandless, E. Feigenbaum, J. Di Nicola, K. Luke, W. Riedel, R. Learn, and B. Kraines, "The virtual beamline (vbl) laser simulation code," in *High Power Lasers for Fusion Research III,* vol. 9345 (SPIE, 2015), pp. 166–183.
16. A. J. Janssen, "Gabor representation and wigner distribution of signals." in *ICASSP,* vol. 84 (1984), pp. 258–261.
17. M. J. Bastiaans, "Gabor's expansion of a signal into gaussian elementary signals," Proc. IEEE **68**, 538–539 (1980).
18. M. Bastiaans, "Wigner distribution function and its application to first-order optics," JOSA **69**, 1710–1716 (1979).
19. J. Weinbub and D. Ferry, "Recent advances in wigner function approaches," Appl. Phys. Rev. **5**, 041104 (2018).
20. D. Dragoman, J. Meunier, and M. Dragoman, "Beam-propagation method based on the wigner transform: a new formulation," Opt. letters **22**, 1050–1052 (1997).
21. R. Simon, E. C. G. Sudarshan, and N. Mukunda, "Gaussian-wigner distributions in quantum mechanics and optics," Phys. Rev. A **36**, 3868–3880 (1987).
22. M. A. Alonso, "Wigner functions in optics: describing beams as ray bundles and pulses as particle ensembles," Adv. Opt. Photonics **3**, 272–365 (2011).
23. M. J. Bastiaans, "Abcd law for partially coherent gaussian light, propagating through first-order optical systems," Opt. quantum electronics **24**, S1011–S1019 (1992).
24. R. Simon, E. C. G. Sudarshan, and N. Mukunda, "Gaussian pure states in quantum mechanics and the symplectic group," Phys. Rev. A **37**, 3028–3038 (1988).
25. L.-g. Wang, Q. Lin, H. Chen, and S.-y. Zhu, "Propagation of partially coherent pulsed beams in the spatiotemporal domain," Phys. Rev. E **67**, 056613 (2003).
26. L. Videau, C. Rouyer, J. Garnier, and A. Migus, "Motion of hot spots in smoothed beams," JOSA A **16**, 1672–1681 (1999).
27. D. Dragoman, "Phase-space interferences as the source of negative values of the wigner distribution function," JOSA A **17**, 2481–2485 (2000).
28. H. T. Stoof, K. B. Gubbels, and D. B. Dickerscheid, *Gaussian Integrals* (Springer Netherlands, Dordrecht, 2009), pp. 15–31.
29. A. Torre, *Linear ray and wave optics in phase space: bridging ray and wave optics via the Wigner phase-space picture* (Elsevier, 2005).
30. R. Simon and N. Mukunda, "Iwasawa decomposition in first-order optics: universal treatment of shape-invariant propagation for coherent and partially coherent beams," JOSA A **15**, 2146–2155 (1998).
31. Worku, Norman G and Hambach, Ralf and Gross, Herbert, "Decomposition of a field with smooth wavefront into a set of Gaussian beams with non-zero curvatures," JOSA A **35**, 1091–1102 (2018).
32. Worku, Norman G and Gross, Herbert, "Gaussian pulsed beam decomposition for propagation of ultrashort pulses through optical systems," JOSA A **37**, 98–107 (2020).
33. Greynolds, Alan W, "Fat rays revisited: a synthesis of physical and geometrical optics with Gaußlets," in *International Optical Design Conference,* vol. 9293 (SPIE, 2014), pp. ITu1A–3.
34. T. Alieva and M. J. Bastiaans, "Properties of the linear canonical integral transformation," JOSA A **24**, 3658–3665 (2007).
35. D. Dragoman, "Higher-order moments of the wigner distribution function in first-order optical systems," JOSA A **11**, 2643–2646 (1994).
36. K.-H. Hong, J.-H. Kim, Y. H. Kang, and C. H. Nam, "Time–frequency analysis of chirped femtosecond pulses using wigner distribution function," Appl. Phys. B **74**, s231–s236 (2002).
37. A. A. Tovar, "Propagation of flat-topped multi-gaussian laser beams," JOSA A **18**, 1897–1904 (2001).
38. C. Fiorini, C. Sauteret, C. Rouyer, N. Blanchot, S. Seznec, and A. Migus, "Temporal aberrations due to misalignments of a stretcher-compressor system and compensation," IEEE journal quantum electronics **30**, 1662–1670 (1994).
39. Worku, Norman G and Gross, Herbert, "Application of Gaussian pulsed beam decomposition in modeling optical systems with diffraction grating," JOSA A **37**, 797–806 (2020).
40. A. Kostenbauder, "Ray-pulse matrices: a rational treatment for dispersive optical systems," IEEE journal quantum electronics **26**, 1148–1157 (1990).
41. J. Paye and A. Migus, "Space–time wigner functions and their application to the analysis of a pulse shaper," JOSA B **12**, 1480–1490 (1995).
42. S. Akturk, X. Gu, P. Gabolde, and R. Trebino, "The general theory of first-order spatio-temporal distortions of gaussian pulses and beams," Opt. express **13**, 8642–8661 (2005).
43. J.-C. Chanteloup, E. Salmon, C. Sauteret, A. Migus, P. Zeitoun, A. Klisnick, A. Carillon, S. Hubert, D. Ros, P. Nickles *et al.*, "Pulse-front control of 15-tw pulses with a tilted compressor, and application to the subpicosecond traveling-wave pumping of a soft-x-ray laser," JOSA B **17**, 151–157 (2000).
44. F. J. Narcowich, "Conditions for the convolution of two wigner distri-

butions to be itself a wigner distribution," J. mathematical physics **29**, 2036–2041 (1988).
45. D. Dragoman, "Wigner distribution function in nonlinear optics," Appl. optics **35**, 4142–4146 (1996).
46. D. Dragoman, "Phase-space formulation of filtering: insight into the wave-particle duality," JOSA B **22**, 633–642 (2005).
47. D. Dragoman, "Wigner distribution function for gaussian–schell beams in complex matrix optical systems," Appl. optics **34**, 3352–3357 (1995).
48. H. Coīc, C. Rouyer, and N. Bonod, "Wigner matrix formalism for phase-modulated signals," JOSA A **38**, 124–139 (2021).